Taylor & Francis
Taylor & Francis Group

RESEARCH PAPER

Linker histone variant H1T targets rDNA repeats

Ruiko Tani*, Koji Hayakawa*, Satoshi Tanaka, and Kunio Shiota

Department of Animal Resource Sciences/Veterinary Medical Sciences, The University of Tokyo, Bunkyo-ku, Tokyo, Japan

ABSTRACT

H1T is a linker histone H1 variant that is highly expressed at the primary spermatocyte stage through to the early spermatid stage of spermatogenesis. While the functions of the somatic types of H1 have been extensively investigated, the intracellular role of H1T is unclear. H1 variants specifically expressed in germ cells show low amino acid sequence homology to somatic H1s, which suggests that the functions or target loci of germ cell-specific H1T differ from those of somatic H1s. Here, we describe the target loci and function of H1T. H1T was expressed not only in the testis but also in tumor cell lines, mouse embryonic stem cells (mESCs), and some normal somatic cells. To elucidate the intracellular localization and target loci of H1T, fluorescent immunostaining and ChIP-seq were performed in tumor cells and mESCs. We found that H1T accumulated in nucleoli and predominantly targeted rDNA repeats, which differ from somatic H1 targets. Furthermore, by nuclease sensitivity assay and RT-qPCR, we showed that H1T repressed rDNA transcription by condensing chromatin structure. Imaging analysis indicated that H1T expression affected nucleolar formation. We concluded that H1T plays a role in rDNA transcription, by distinctively targeting rDNA repeats.

Abbreviations: ChIP, chromatin immunoprecipitation; ERV, endogenous retrovirus; ETS, external transcribed spacer; GD, globular domain; HAEC, human aortic endothelial cell; hRPTEC, human renal proximal convoluted tubule epithelial cell; IGS, intergenic space; ITS, internal transcribed spacer; LTR, long terminal repeat; MBEC, mammary basal epithelial cell; mESCs, mouse embryonic stem cells; MLEC, mammary luminal epithelial cell; MNase, Micrococcal nuclease; NAD, nucleolus-associated chromatin domain; N.D., not detected; NT, non-treated; NTD, N-terminal domain; SkMC, human skeletal muscle cell; SnRNA, small nuclear RNA; TSS, transcriptional start site

Introduction

The structural unit of chromatin, the nucleosome, consists of an octamer of core histones (H2A, H2B, H3, and H4) surrounded by 146 base pairs of genomic DNA and a varied length of linker DNA bound by linker histone H1.[1,2] Compared to core histones, linker histone H1 is not as conserved through evolution.[3] Mammals have ten H1 variants and one H1-like protein (HILS1), which are classified, according to their expression patterns, into two groups: somatic variants (H1A, H1B, H1C, H1D, H1E, H1F0, and H1FX) and germ cell-specific variants (H1FOO, H1T, H1FNT, and HILS1).[4-6] H1FOO is an oocyte-specific variant,[7,8] and H1T, H1FNT, and HILS1 are testis-specific.[9-12]

H1 is closely associated to epigenomic events since it remodels chromatin structures.[13,14] According to studies on H1 somatic variants, H1 is commonly thought to condense chromatin structures, which leads to the packaging of genomic DNA in the nucleus and the repression of gene expression. However, we previously found that H1foo has a different function from that of other H1 variants; it decondenses chromatin structures at pluripotent- and oocyte-related genes, which contributes to chromatin structure

relaxation.[15] H1 is composed of 3 domains: a short N-terminal domain (NTD), a central globular domain (GD) that contains DNA-binding sites, and a long C-terminal domain (CTD).[16,17] Of these, NTD and CTD show variation in amino acid sequences among H1 variants,[18] with germ cell-specific variants having relatively low homology to H1A, H1B, H1C, H1D, and H1E, as shown in the phylogenetic tree of human H1 variants (Fig. S1).[19] This low homology between amino acid sequences suggests that germ cell-specific variants may possess functions and target loci different from those of somatic variants.

H1T starts to be synthesized from the meiotic spermatocyte stage of spermatogenesis and accounts for 40% of the total H1 in the cells.[20,21] In humans, H1T is expressed until the late spermatid stage [21] and, in mice, H1t is detected until the early spermatid stage.[22,23] H1t knockout mice have no apparent phenotype in spermatogenesis due to the compensatory upregulation of somatic H1s.[24,25] This has favored the idea that the function of H1T is redundant as it overlaps with that of somatic types. However, a previous report showed that specific repression of somatic H1 variants in cancer cells by knockdown could reveal their unique

intracellular roles,[26] implying that there is functional specificity for each variant. The amino acid sequence of H1T differs from that of somatic H1. For example, H1T lacks the SPKK-motif in the CTD, which works as a minor DNA binding motif and contributes to chromatin condensation.[27,28] This suggests that H1T may have a unique function that differs from somatic H1s. Until now, there has been no report on the target loci and biological function of H1T.

In this study, we present the expression profile of germ cell-specific H1 variants in non-germ cells, such as human cancer cells and normal somatic cells. Moreover, since H1T was expressed in most tumor cell types, we further studied the characteristics of H1T using these cells. We found that H1T is accumulated in the nucleoli and that it uniquely targets rDNA repeating units.

Results

Gene expression of germ cell-specific H1 variants

While studying H1foo using mouse embryonic stem cells (mESCs), we obtained preliminary data indicating that *H1t* was expressed in mESCs, but its expression was significantly decreased after differentiation (Fig. 1A and B), suggesting that germ cell-specific H1s are not limited to germ cells only. To elucidate the gene expression of germ cell-specific H1 variants (*H1T, H1FNT,* and *H1FOO*) in other cell types, we examined a variety of cells, including eight human cancer cell lines (gastric cancer cells: AGS, HSC-39, HSC-57, and KATOIII; duodenal cancer cells: HuTu80; and breast cancer cells: MDA-MB-231, MCF-7, and YMB-1) and non-cancerous somatic cells [mammary basal epithelial cells (MBECs), mammary luminal epithelial cells (MLECs), human renal proximal convoluted tubule epithelial cells (hRPTECs), human aortic endothelial cells (HAECs), skeletal muscle cells (SkMCs), and stomach] by RT-PCR analyses. *H1T* and *H1FNT* were expressed in the testis while *H1FOO* was not (Fig. 1C), supporting previous reports.[7-11] It is important to note that the expression of *H1T* was also detected in stomach and cancer cell lines, including KATOIII, MDA-MB-231, MCF-7, and YMB-1. In addition, weak bands were detected in other cell types. *H1FNT* expression was also detected in the MCF-7 line, and *H1FOO* expression was observed in YMB-1 and MBEC cells.

The expression of *H1T* was further analyzed by RT-qPCR (Fig. 1D). The expression level was confirmed in all breast cancer cell lines, with the highest expression being found in MCF-7 cells. Of the gastric cancer cell lines, KATOIII showed the highest expression level, and AGS and HSC-39 showed the lowest. *H1T* expression varied between cell lines.

Localization of H1T in nucleoli of human cells

To estimate the expression and intercellular localization of H1T protein in non-germinal cells, immunostaining of H1T was performed in human cells (Fig. 2A). In MCF-7 and HSC-57 cells, H1T was localized in both nuclei and cytoplasm. On the other hand, in AGS, HuTu80, MDA-MB-231, HSC-39,

KATOIII, YMB-1, and SkMC cells, H1T was detected predominantly in nuclei. MDA-MB-231, MCF-7, HSC-39, HSC-57, and KATOIII cells showed diffused H1T localization in nucleoplasm. Considering a IgG-stained image as a negative control, expression of H1T could not be observed in MBEC, MLEC, and HAEC, where mRNA expression of *H1T* was lower or hardly detectable. Taken together, the expression of H1T protein was confirmed in non-germ cells, which implies that H1T has a function in these cells.

More precise observation of immunostaining images indicated that a particular region of the nucleus was strongly stained with α-H1T in all cancer cell lines and SkMC. This area showed little DAPI staining, suggesting the H1T was accumulated in the nucleolus. We double-stained cells with α-H1T and an antibody against nucleophosmin (α-B23), a marker of the nucleolus and confirmed that H1T co-localized with nucleophosmin. On the other hand, the intracellular localization of somatic H1 variant H1C differed from that of H1T; H1C showed various localization patterns (Fig. S2). AGS, HuTu80, HAEC, and SkMCs showed overall H1C nuclear localization and nucleolar accumulation that was slightly or much less distinctive than that of H1T. In MDA-MB-231 and MCF-7, H1C was localized to the nucleoplasm except inside nucleoli. Thus, the consistency in its nucleolar accumulation characterized the localization of H1T.

To assess the cell cycle dependence of H1T localization, AGS cells were cultured and their cell cycles were synchronized. Cells at each stage of the cell cycle were then immunostained for H1T (Fig. 2B). Nucleolar localization of H1T was observed at all cell cycle stages except metaphase. Collectively, immunostaining results clearly demonstrated that H1T protein accumulated in the nucleoli regardless of cell type and cell cycle.

Biased distribution of H1T to rDNA in cancer cell lines

To investigate the distribution of H1T within genomic DNA, chromatin immunoprecipitation (ChIP)-seq was performed in AGS and MDA-MB-231 cells using α-H1T. Some somatic H1 variants show unique distributions on repeat sequences.[29,30] At first, each ChIP-seq library was mapped on the whole human genome to calculate the mapping ratio to multi-positions or unique sequences (Fig. S3A). While sheared chromatin input control libraries from AGS and MDA-MB-231 cells had 19.4% and 22% of reads mapped to multi-positions, respectively, H1T ChIP-seq libraries of the same cell lines had 32.6% and 31.4% mapped to multi-positions, respectively. This observation suggested that, like some somatic H1 variants (Fig. S3A), a higher proportion of H1T was localized to repetitive sequences.

The nucleolus, where H1T is predominantly localized, contains various types of repeat sequences, such as rRNA- and tRNA-coding sequences.[31] Therefore, the sequencing data were mapped to the repeat libraries in Repbase (version 18.11).[32] H1T was mostly associated with pseudogenes and CpG islands in repeat sequences (Fig. 3A). Compared to the localization of somatic type of H1 variants (H1C, H1E, H1F0, and H1FX) in human breast cancer cell line T47D,[33] H1T showed lower localization to DNA transposon, endogenous retrovirus (ERV) and long-terminal repeats (LTRs). On the other hand, H1T showed
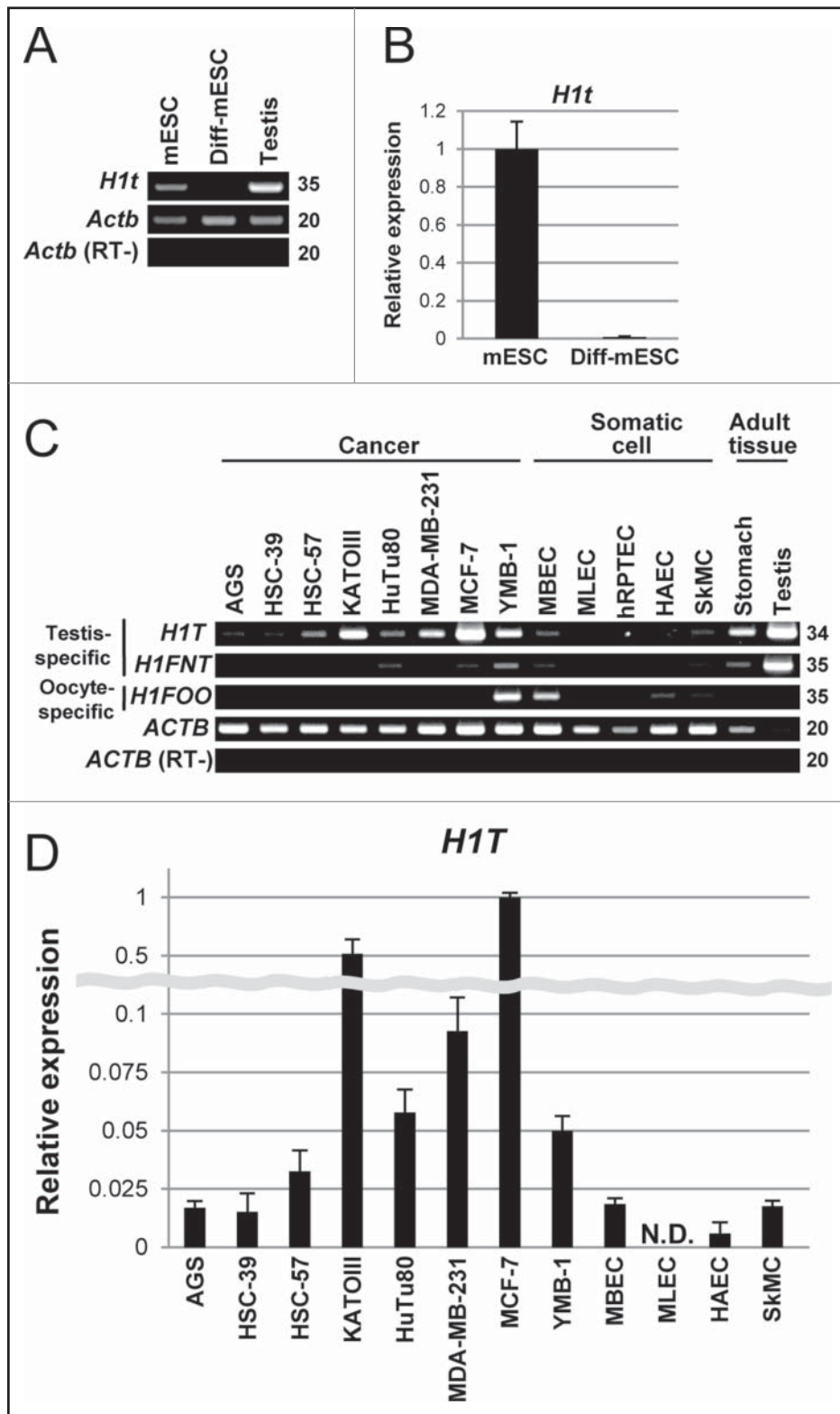
Figure 1. Germ cell-specific H1 variants were expressed in various cell types. (A) Expression of *H1t* in mouse embryonic stem cells (mESCs), determined by RT-PCR. For induction of differentiation (Diff), mESCs were cultured without LIF for 6 d. Expression of *Actb* was used as an internal control. The number of cycles in RT-PCR experiment for each gene is shown on the right side. RT- was synthesized without reverse transcriptase enzyme. Testis RNA was used as a positive control. (B) Expression of *H1t* in mESCs by RT-qPCR. Values are means ± SD derived from 3 independent qPCR reactions, were normalized to the expression of *Actb*, and were indicated relative to mESCs. (C) Expression analysis of germ cell-specific H1 variants in human cells and tissues by RT-PCR. AGS, HSC-39, HSC-57, and KATOIII are human gastric cell lines. HuTu80 is a human duodenal cancer cell line. MDA-MB-231, MCF-7, and YMB-1 are human breast cancer cell lines. MBEC, mammary basal epithelial cell. MLEC, mammary luminal epithelial cell. hRPTEC, human renal proximal convoluted tubule epithelial cell. HAEC, human aortic endothelial cell. SkMC, skeletal muscle cell. Testis RNA was used as a positive control to testis-specific variants. Expression of *ACTB* was used as an internal control. The number of cycles in RT-PCR experiment for each gene is shown on the right of each part. RT- was synthesized without reverse transcriptase enzyme. (D) Measurement of *H1T* expression level by RT-qPCR. Values are means ± SD derived from 3 independent qPCR reactions, were normalized to the expression of *ACTB*, and were indicated relative to MCF-7. N.D., not detected.
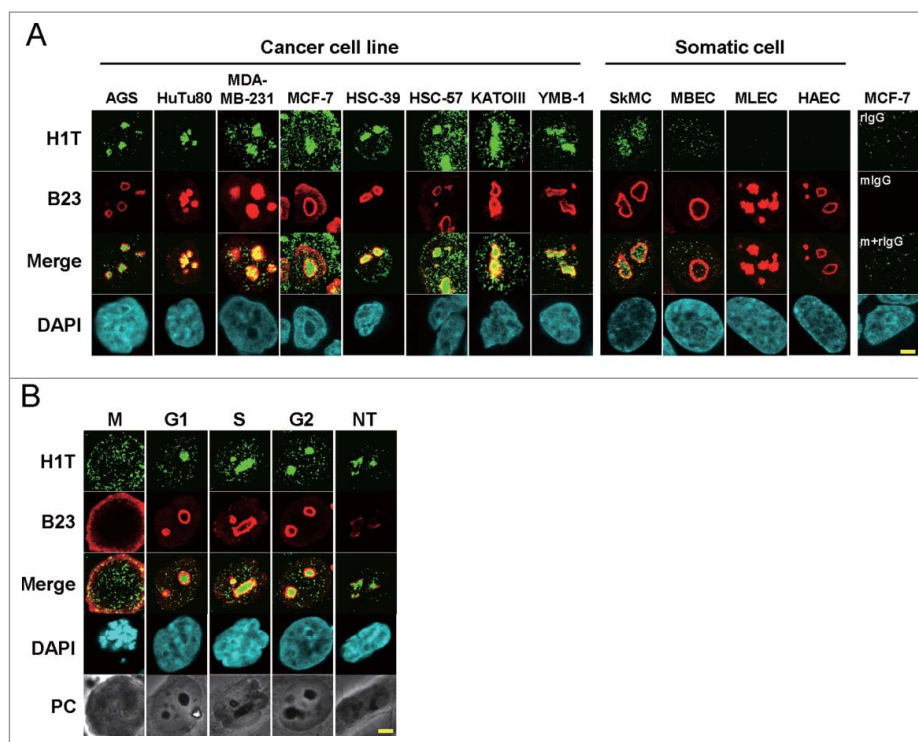
Figure 2. H1T was localized in nucleoli. (A) Fluorescent immunostaining of H1T (green) and B23 (red) in human cancer cell lines and somatic cells. Rabbit and mouse Immunoglobulin G (rIgG and mIgG) was used as a negative control. Scale bars, 4 μm. (B) Fluorescent immunostaining of H1T (green) and B23 (red) in cell-cycle-synchronized AGS. Cell cycles were synchronized at S phase (S) by thymidine, and then were stopped by nocodazole for G2 phase (G2) and metaphase (M), by mimosine for G1 phase (G1). NT, non-treated. PC, phase contrast. Scale bars, 4 μm.

a higher localization to pseudogenes compared to somatic variants. This biased distribution to pseudogenes was unique to H1T.

According to the classification by Repbase, pseudogenes consist of rRNA, snRNA, and tRNA coding regions. H1T preferably localized to rRNA-coding loci as compared to somatic variants (Fig. 3B). ChIP-seq data were also mapped for rDNA repeating units (GenBank U13369), which consist of transcribed regions (47S pre-rRNA coding loci) and intergenic spaces (IGS). H1T was predominantly associated with pre-rRNA coding loci (Fig. 3C).

Distribution of H1T within the rDNA repeating unit in cancer cell lines

To examine the binding of H1T within the rDNA repeating unit in more detail, ChIP-qPCR analyses were performed. For comparison, the distribution of H1C was also examined. Before
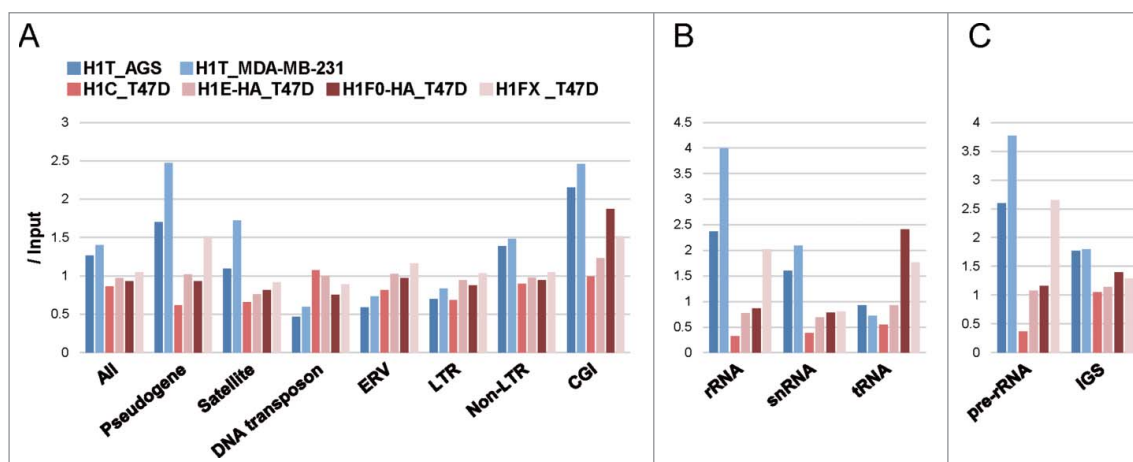

Figure 3. H1T preferably bound with rDNA repeating units compared with somatic H1 variants in cancer cell lines. (A) Distribution of human H1 variants on repeat sequences. Chromatin immunoprecipitation (ChIP)-seq data were mapped to repeat sequence libraries in Repbase (ver. 18.11). Enrichment of H1s was normalized by the data of input DNA. ERV, an endogenous retrovirus. LTR, long terminal repeat. CGI, CpG island. (B) Distribution of human H1 variants on repeat sequences categorized in pseudogenes. snRNA, small nuclear RNA. (C) Distribution of human H1 variants on rDNA repeating unit. ChIP-seq data were mapped onto human rDNA repeating units (GenBank U13369). IGS, intergenic space.
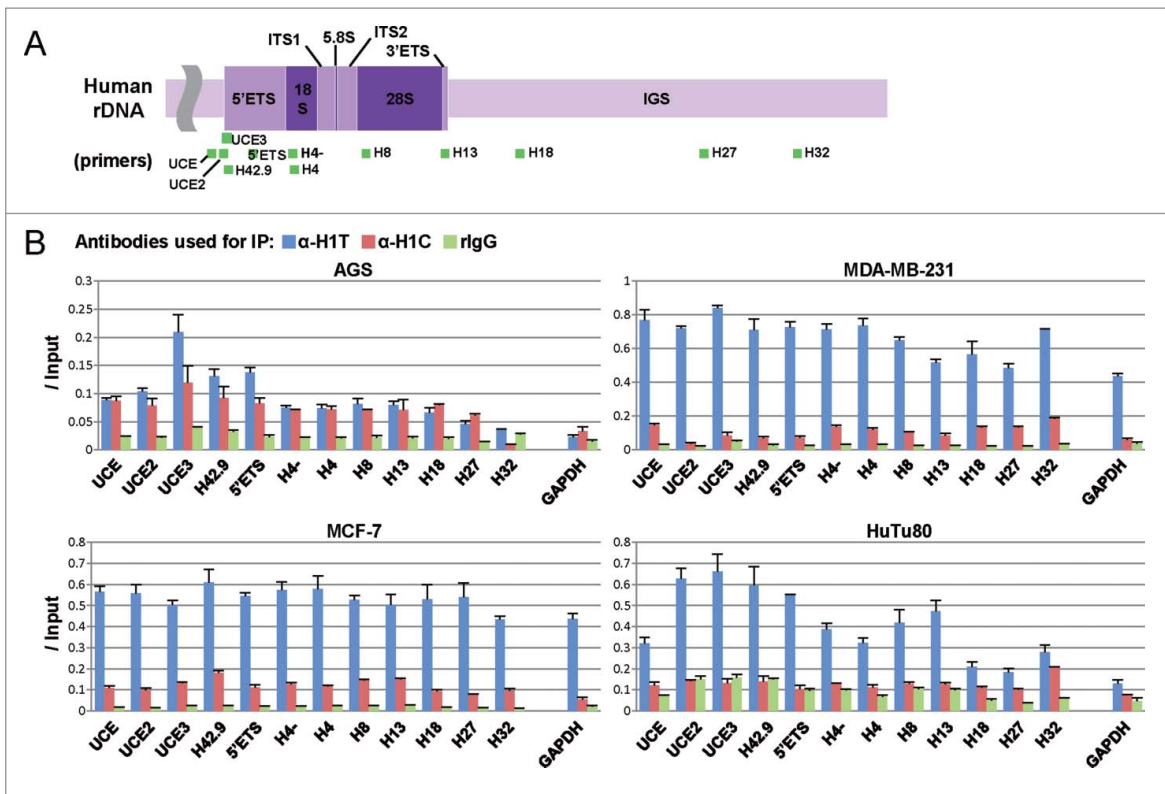
Figure 4. H1T was bound to rDNA repeating units in cancer cell lines. (A) Diagram of a human rDNA repeat. qPCR amplicons were indicated as green bars. ETS, external transcribed spacer. ITS, internal transcribed spacer. (B) H1T and H1C profile over rDNA repeating unit by ChIP-qPCR in AGS, MDA-MB-231, MCF-7 and HuTu80 cells. *GAPDH* gene locus was used as a control region. Values are means ± SD derived from three independent qPCR reactions and were normalized to input signal. IP, immunoprecipitation.

the analysis on rDNA repeating units, we performed ChIP-qPCR analysis focusing on H1C-enriched loci detected and selected based on previous ChIP-seq data for H1C (*CRYGS, OPA1, ABCA6, SLC16A7, LINC0057, POU6F2, GAS2, OR8B3, EGFEM1P, KCNT2,* and *PYDC2*)[33] (Fig. S4). The ratio of α-H1C-immunoprecipitated DNA to input DNA was higher than or almost equal to that of α-H1T-immunoprecipitated DNA. Therefore, for the analysis on rDNA repeating units by ChIP-qPCR, we ruled out the possibility that the titer of α-H1C antibody was too low to be detected in H1C-enrichment compared to α-H1T.

Next, we prepared 12 primer sets targeting the rDNA repeating unit (Fig. 4A)[34] and AGS, MDA-MB-231, MCF-7 and HuTu80 cells were subjected to ChIP-qPCR using α-H1T and α-H1C (Fig. 4B). In AGS cells, biased distribution of H1T was observed at the *UCE3* locus, although the ratios of immunoprecipitated DNA to input DNA were almost the same between H1T and H1C at the other loci. MDA-MB-231 and MCF-7 cells showed H1T enrichment over the entire repeating unit, particularly around the TSS (UCE, UCE2, UCE3, H42.9, and 5′ETS). In HuTu80 cells, H1T was distributed predominantly in the transcribed region. H1T distribution was more biased toward TSS in AGS and HuTu80 cells than in MDA-MB-231 and MCF-7 cells. Although the distribution pattern differed depending on the cell line, H1T was intensively localized over the rDNA repeating unit, particularly at its TSS.

To further strengthen the data showing the specificity of H1T to rDNA, we performed ChIP-qPCR using anti-Flag antibody in AGS and MDA-MB-231 cells, in which 3xFlag (Flag-

control) or 3xFlag-tagged H1T (Flag-H1T) was stably overexpressed (Fig. S5A). As expected, Flag-H1T-overexpressing cell lines showed enrichment of Flag-H1T over the rDNA repeating unit, compared to control cell lines (Fig. S5B).

Biased distribution of H1t at rDNA in mESCs

Immunostaining of mESCs showed that H1t was mainly localized to nucleoli, different form H1c (Fig. 5A and B). Furthermore, intracellular localization of H1t was also examined in mouse spermatogenic cells, since H1t was originally discovered as a protein that is highly expressed in the testis.[9,10] Fluorescent immunostaining of spermatogenic cells for H1t and Scp3, a marker of meiosis, revealed that, in spermatocytes, H1t was not equally diffused throughout the nucleus, but was accumulated at some foci, whereas in spermatids it showed lower overall expression and diffused localization (Fig. 5C). B23 protein (nucleophosmin) was localized in the nucleoli of spermatogenic cells as well as somatic cells.[35] To elucidate whether H1t was localized to the nucleolus, spermatogenic cells were co-immunostained with α-H1T and α-B23 (Fig. 5D). Images of spermatocytes were selected according to the comparison of DAPI-stained images with those in Fig. 5C. Accumulation of H1t immunostaining colocalized with that of B23 immunostaining in spermatocytes, which indicated nucleolar localization of H1T. In addition, some α-H1T-stained particles did not merge with the α-B23-stained regions. Collectively, tumor cell lines, mESCs, and germ cells show nucleolar localization of H1t.
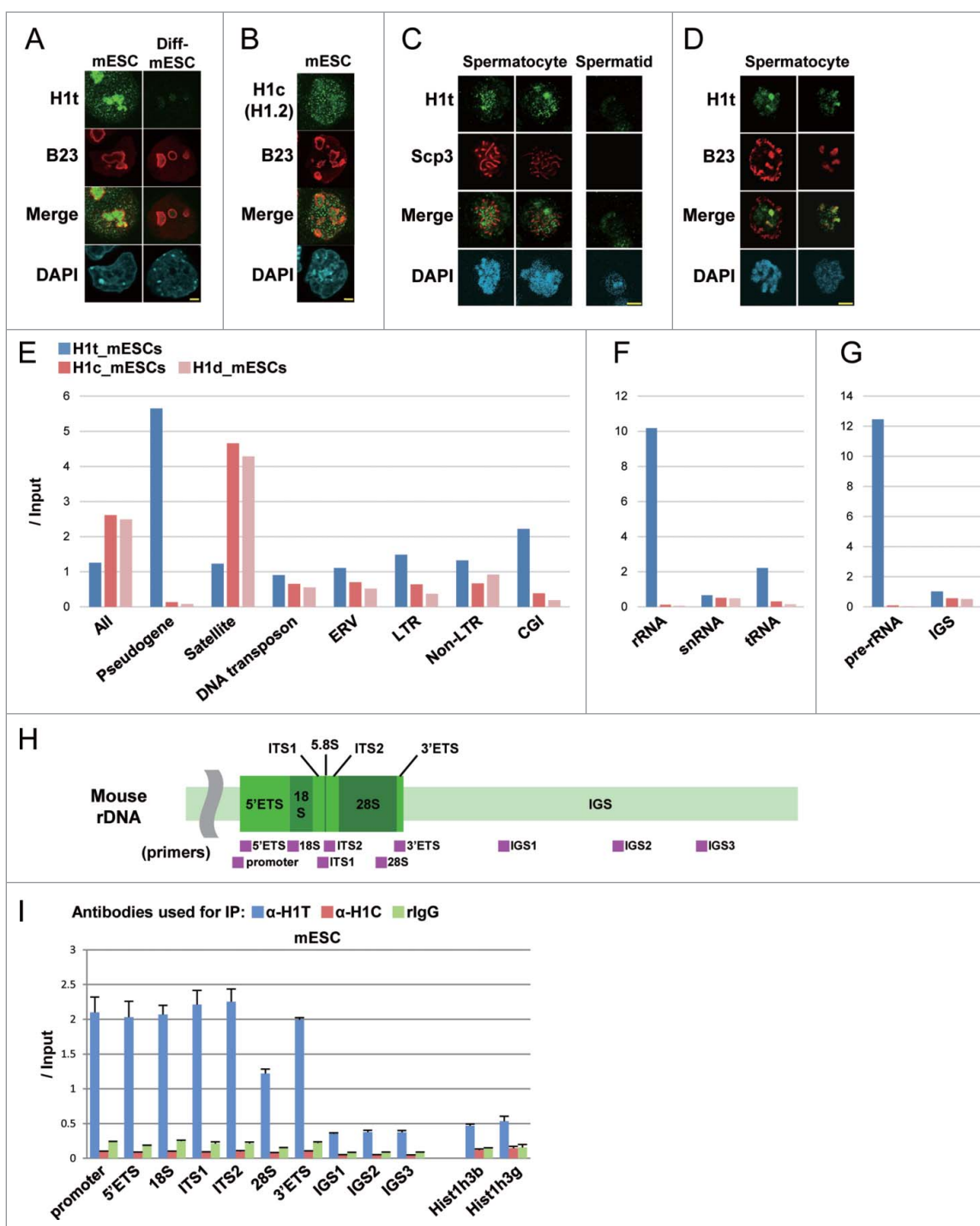
Figure 5. H1t targeted rDNA in mESCs. (A) Fluorescent immunostaining of H1t and B23 in mESCs. Cells were stained with α-H1T (green), α-B23 (red), and DAPI (cyan). B23 antibody was used as a maker of nucleoli. Merge, a merged image of H1t and B23. Scale bars, 2 μm. (B) Fluorescent immunostaining of H1c and B23 in mESCs. Cells were stained with α-H1c (green), α-B23 (red) and DAPI (cyan). Merge, a merged image of H1c and B23. Scale bars, 2 μm. (C) Fluorescent immunostaining of H1t and Scp3 in mouse spermatogenic cells. Cells were stained with α-H1T (green), α-Scp3 (red), and DAPI (cyan). The Scp3 antibody was used as a marker of meiosis. Merge, a merged image of H1T and Scp3. Scale bars, 5 μm. (D) Fluorescent immunostaining of H1t and B23 in mouse spermatocytes. Cells were stained with α-H1T (green), α-B23 (red), and DAPI (cyan). Merge, a merged image of H1T and B23. Scale bars, 5 μm. (E) Distribution of mouse H1 variants on repeat sequences. (F) Distribution of mouse H1 variants on repeat sequences categorized in pseudogenes. (G) Distribution of mouse H1 variants on rDNA repeating unit. ChIP-seq data were mapped onto mouse rDNA repeating units (GenBank BK000964). (H) Diagram of a mouse rDNA repeat. qPCR amplicons were indicated as purple bars. (I) H1t and H1c profile over rDNA repeating unit by ChIP-qPCR. *Hist1h3b* and *Hist1h3g* gene locus were used as control regions. Values are means $\pm$ SD derived from three independent qPCR reactions and were normalized to input signal.

mESCs were also subjected to ChIP-seq using α-H1T for comparison with the published ChIP-seq data of somatic H1 variants (H1c and H1d).[29] As observed in human cancer cells, in mESCs, a higher percentage of multi-position sequence reads (30.6% of total mapped reads on the mouse genome) was observed in the ChIP-seq library for H1t than that for input (Fig. S3B). The ChIP-seq libraries for H1c and H1d showed biased mapping to multi-positions, because these H1s mainly

localize to major satellite sequences.[29] Again, the sequencing data were mapped to the repeat libraries in Repbase (Fig. 5E). H1t was primarily associated with pseudogenes among repeat sequences in mESCs, a feature that is unique to H1t. Moreover, H1t predominantly bound to rRNA-coding regions compared to somatic H1 variants (Fig. 5F). ChIP-seq data mapped to rDNA repeating unit (GenBank BK000964) showed that H1t bound more to transcribed regions than to IGS (Fig. 5G). By ChIP-qPCR using the primers constructed for sequences within the rDNA repeating unit (Fig. 5H), we confirmed that H1t bound more to transcribed regions than IGS (Fig. 5I).

Taken together, ChIP-seq and ChIP-qPCR analyses revealed that H1T specifically binds to rRNA coding region in several cancer cell lines and mESCs, unlike somatic H1 variants.

Chromatin condensation of rDNA repeats by H1T

To clarify how H1T would affect chromatin structures, DNase I sensitivity assays were performed focusing on rDNA in Flag-H1T-overexpressing AGS, MDA-MB-231, and MCF-7 cell lines (see, Fig. S5A). Overexpression of Flag-H1T caused chromatin condensation of rDNA, especially around TSS (UCE, UCE2, UCE3, and H42.9) in all Flag-H1T-expressing cell lines (Fig. 6A). To strengthen the results of the DNase I sensitivity assay, we prepared MNase-digested chromatin and measured nucleosome occupancy on rDNA repeats. qPCR using DNA purified from MNase-digested chromatin showed that nucleosome occupancy

increased over the rRNA-coding region (UCE~H13) in all Flag-H1T-expressing cell lines compared to control cell lines (Fig. 6B). These results suggest that localization of H1T to rDNA regions contributes to the repression of rDNA transcription.

RT-qPCR revealed that the expression level of pre-rRNA was significantly decreased by Flag-H1T overexpression in AGS and MDA-MB-231 cells, and had a tendency to be lower in MCF-7 cells, compared to control cell lines (Fig. 7A). Overexpression of Flag-H1T significantly suppressed cell proliferation in AGS cells and had a tendency to suppress cell proliferation in MDA-MB-231 and MCF-7 cells (Fig. 7B). In contrast, knockdown of H1T by miRNA resulted in increased expression of pre-rRNA in AGS, MDA-MB-231, and MCF-7 cells (Fig. 7C and D). These overexpression and knockdown studies clearly indicate that H1T plays a role in the repression of rDNA transcription in these cancer cell lines.

Repressive role of H1T in nucleolar constitution

The nucleolus is a non-membrane-bound nuclear structure that harbors the genes for rRNA (rDNA) and where their transcription occurs. The localization of H1T in the nucleoli of some non-germ cells, including tumor cell lines, and the condensation of the chromatin structures at rDNA regions prompted us to examine the relationship between H1T and the nucleolar constitution. Nucleoli of Flag-H1T-overexpressing MDA-MB-231 and MCF-7 cell lines were visualized by immunostaining with α-B23 and the area of each nucleolus was measured. The
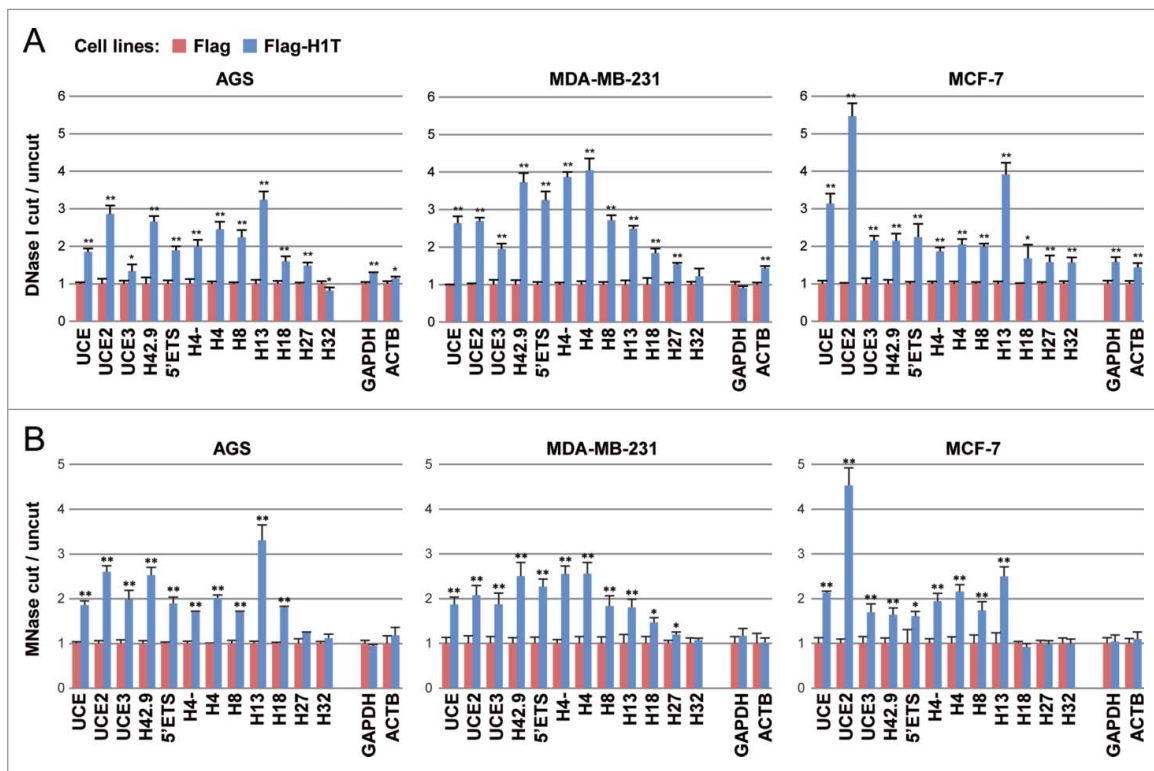

Figure 6. H1T induced condensation of chromatin at rDNA. (A) DNase I sensitivity assay of H1T-overexpressing AGS, MDA-MB-231, and MCF-7 cells. Chromatin of Flag-(control) and Flag-H1T-overexpressing AGS, MDA-MB-231, and MCF-7 cells (see Fig. S5A) was digested with DNase I and examined by qPCR. DNA purified from digested chromatin samples (cut), and undigested chromatin samples (uncut) was amplified using primer sets designed over the rDNA repeating unit (see Fig. 4A). *ACTB* and *GAPDH* gene locus were used as control regions. Values were calculated as cut/uncut, and expressed as means ± SD derived from 3 independent qPCR reactions, and were indicated relative to value of control cell lines. *, $P < 0.05$. **, $P < 0.01$ (Student's t-test). (B) MNase sensitivity assay of H1T-overexpressing AGS, MDA-MB-231, and MCF-7 cells. Chromatin of Flag- (control) and Flag-H1T-overexpressing AGS, MDA-MB-231, and MCF-7 cells was digested with MNase and examined by qPCR.
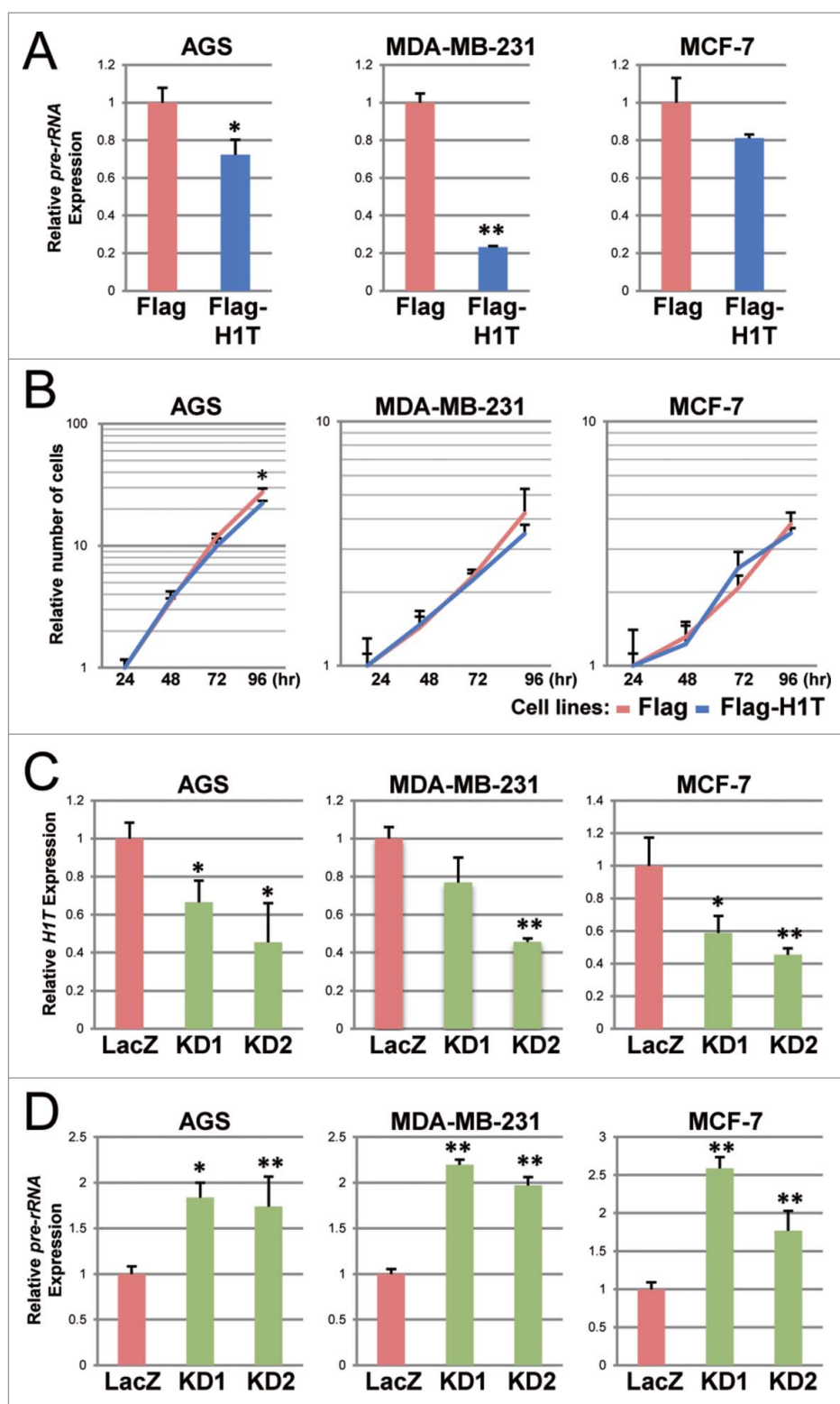
Figure 7. H1T repressed rDNA transcription. (A) Expression analysis of pre-rRNA in Flag-H1T-overexpressing cells by RT-qPCR. Overexpression of Flag-H1T was confirmed in Fig. S5A. Values are means ± SD derived from three independent qPCR reactions, normalized to the expression of *ACTB*, and indicated relative to Flag. *, $P < 0.05$. **, $P < 0.01$ (Student's t-test). (B) Cell proliferation in Flag-H1T-overexpressing cells. The number of cells was indicated relative to that counted at 24 hr. Experiments were carried out in triplicate. *, $P < 0.05$ (Student's t-test). (C) Preparation of H1T knockdown (K_D) samples. Cells transiently (AGS) or stably (MDA-MB-231 and MCF-7) expressed miRNA for H1T K_D (KD1 and KD2) or for LacZ K_D (LacZ) as a control. H1T K_D was checked by RT-qPCR. Values are means ± SD derived from three independent qPCR reactions, normalized to the expression of *ACTB*, and indicated relative to LacZ. *, $P < 0.05$. **, $P < 0.01$ (Student's t-test). (D) Expression analysis of pre-rRNA in H1T K_D cells by RT-qPCR. Values are means ± SD derived from three independent qPCR reactions, normalized to the expression of *ACTB*, and indicated relative to LacZ. *, $P < 0.05$. **, $P < 0.01$ (Student's t-test).
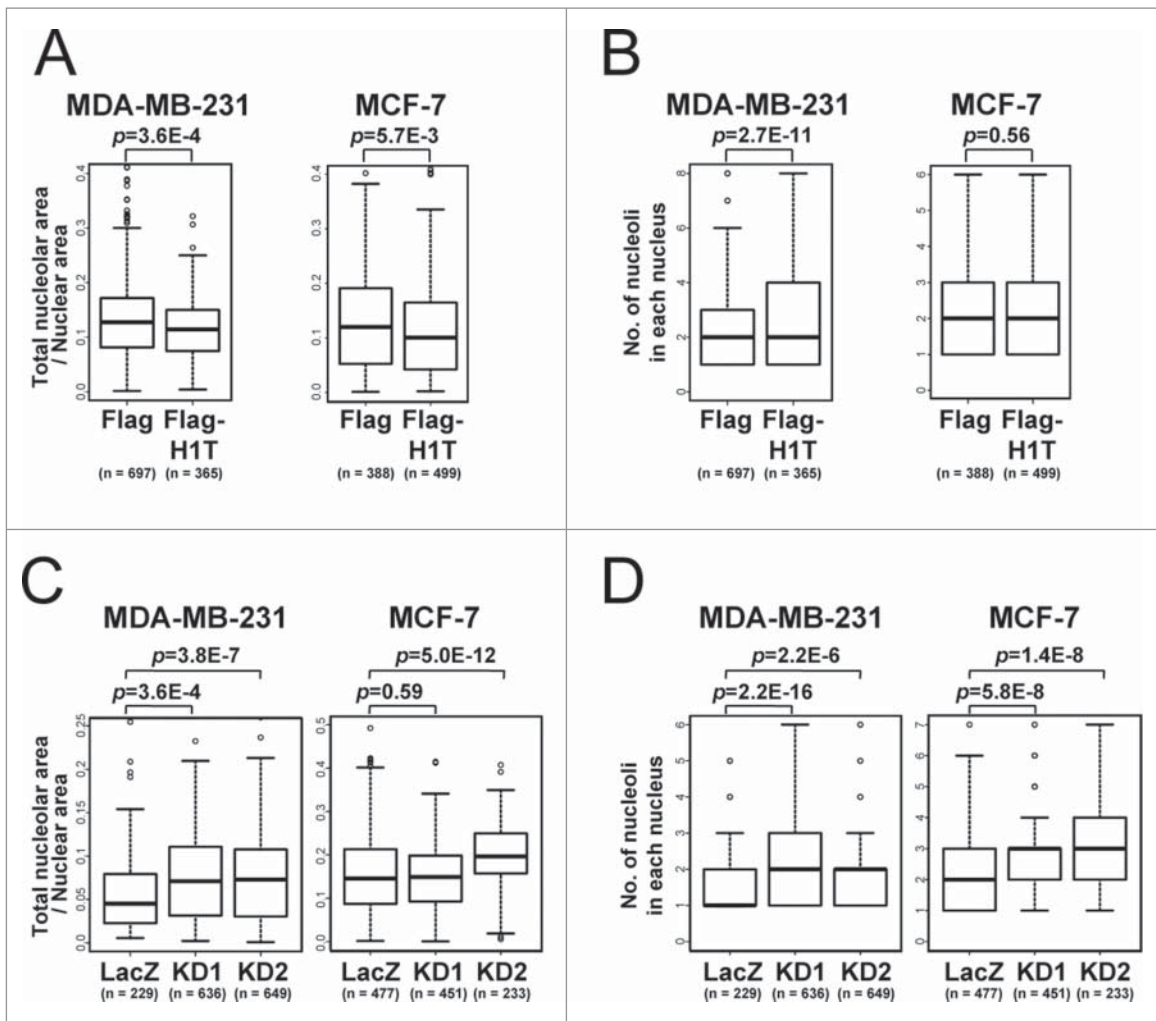
Figure 8. H1T induced decrease in nucleolar size. (A) Proportion of total area of nucleoli in each nucleus to nuclear area in Flag-H1T-overexpressing cells. In fluorescent immunostaining, nucleoli and nuclei were visualized by an antibody against B23 and by DAPI, respectively. Each area was measured by Cell Profiler.[58] P-values were calculated through Wilcoxon rank-sum test. (B) Number of nucleoli in each nucleus in Flag-H1T-overexpressing cells. Counting was performed by Cell Profiler. (C) Proportion of total area of nucleoli in each nucleus to nuclear area in H1T K_D cells. (D) Number of nucleoli in each nucleus in H1T K_D cells.

size of nucleoli was significantly reduced by Flag-H1T overexpression in both cell types (Fig. S6A). The proportion of total nucleolar area to nuclear area in each nucleus was also calculated (Fig. 8A, S6A, and S6B). These results further suggest that H1T functioned to decrease nucleolar size. Additionally, the number of nucleoli inside each nucleus was counted and no change between control and Flag-H1T-overexpressing cell lines was observed (Fig. 8B). In H1T-knockdown cell lines (see, Fig. 7C), nucleolar size was larger than in control lines (Fig. 8C, S6C, and S6D). Moreover, the number of nucleoli was increased by H1T knockdown (Fig. 8D). Taken together, H1T appears to condense chromatin at rDNA repeats, which leads to repressed rDNA transcription and decreased nucleolar size.

Discussion

In the present study, we found that linker histone variant H1T is expressed not only in the testis but also in non-germ cells, including cancer cells and mESCs. In non-germ cells, H1T has a biological function even though its expression is lower than that in the testis. H1T targets rDNA repeat units and represses

pre-rRNA transcription by condensing chromatin structure. Moreover, H1T decreases the number and size of nucleoli. H1T fulfills the same function in chromatin remodeling as somatic H1 variants do. However, H1T target loci differ from those of H1 somatic variants.

Fluorescent immunostaining showed that H1T accumulated in the nucleoli of cancer cell lines, SkMCs, mESCs, and mouse spermatocytes. Other reports indicate that H1 variants also show nucleolar localization. In human embryonic stem cells (hESCs), H1A was predominantly localized to nucleoli and H1B, H1C, and H1D showed 2 localization patterns: nucleolar and diffuse nuclear localization.[36] H1C and H1E were also reported to accumulate in nucleoli when phosphorylated during interphase in HeLa S3 cells.[37] H1FX accumulates in nucleoli during G1 phase and becomes evenly distributed in the nucleus during S and G2 phases.[38] These previous reports indicate that nucleolar localization of somatic variants is dependent on cell type and cell cycle stage. On the other hand, H1T shows nucleolar accumulation regardless of cell type and cell cycle stage. Therefore, our data suggest that H1T has a different function

in nucleoli from somatic H1s and that it constantly expresses its cellular function in nucleoli.

In addition to nucleolar accumulation, we demonstrated that H1T targets rDNA repeats and that this biased targeting is unique to H1T on the genome. A recent report indicated that H1FX and H1F0 were localized to rDNA repeats.[30] H1FX and H1F0 were mainly enriched in a region of the rRNA-coding sequence and IGS, respectively. Since H1T was mainly localized over the entire rRNA-coding region in the cells examined, the target loci of H1T partially overlap those of H1FX, but are segregated from those of H1F0 in rDNA units. Moreover, H1FX and H1F0, but not H1T, were highly associated with tRNA-coding loci in this study. The nucleolus contains not only rDNA repeats but also other genomic regions. A detailed analysis of nucleolus-associated chromatin domains (NADs) revealed that NADs are contained in specific sequences, such as satellite repeats, immunoglobulin-protein-coding gene families, transcriptionally active 5S RNA genes, and tRNA genes.[31] Thus, even though H1T and somatic H1 variants are both localized to nucleoli, they appear to have different target loci and play different roles inside nucleoli.

Here, we found that H1T was expressed and functioned in all human cancer cell lines examined, even with much lower expression level than in testis. Almost 25 y ago, cancer testis antigens were identified as tumor antigens encoded by genes that are normally expressed only in germ cells.[39-42] In the present study, H1T could be identified as a cancer testis antigen. Since H1T was expressed in all cancer cell lines examined in our study—gastric cancer, duodenal cancer, and breast cancer—, H1T is expected to be an antigen against various kinds of tumors.

In addition to cancer cell lines, H1T expression is also observed in SkMCs and mESCs. SkMCs are myoblast cells, which are not terminally differentiated and have potential for differentiation. H1t expression level in differentiated mESCs was greatly decreased. These H1T-expressing non-germ cells are all in an undifferentiated state and share high proliferation potency. Curiously, however, H1T functions against proliferation potency in these non-germ cells; Flag-H1T-overexpressing cell lines proliferate slower than control lines, and H1T represses rDNA transcription. Moreover, H1T appears to repress nucleolar constitution in tumor cells, which typically present abnormal (larger) nucleolar size and greater number of nucleoli than normal cells.[43,44] The level of ribosomal biogenesis, including rDNA transcription, is positively correlated with cell proliferation, and this biogenesis is essential to express unique cellular functions.[45] Therefore, rRNA production must be controlled to suitable levels for cells to avoid aberrant protein synthesis. Indeed, even in tumor cells, not only proliferation-inducing phenotypes but also anti-proliferative factors can be observed; the rDNA locus has a tendency to be hypermethylated in tumors as compared to normal breast tissue.[46] Considering these observations, we conclude that H1T may act in proliferative cells, such as tumor cells and stem cells, to avoid excessive protein synthesis by repressing rDNA transcription.

During spermatogenesis, the rate of rRNA synthesis changes;[47,48] rRNA is highly synthesized in spermatogonium, and its synthesis increases from the prophase stage of first meiosis. The rate of synthesis is highest at mid-pachytene stage and then progressively decreases as spermatogenesis continues to the spermatid stage. The present study revealed that H1T is localized to the nucleoli of mouse spermatocytes, which implies that H1T targets rDNA repeats in germ cells as well as non-germ cells. Considering this result and a previous report on the expression profile of H1t during spermatogenesis,[9,10,20-25] H1t is expressed in spermatogenic cells when rRNA is highly synthesized. Therefore, as in non-germ cells, H1t might target rDNA repeating units also in spermatogenic cells and control pre-rRNA expression.

In terms of condensing chromatin structures, H1T has the same function as somatic H1 variants while H1foo has the opposite function.[15] In the phylogenic tree of H1 variants (Fig. S1), H1FOO is mapped at the almost direct opposite position to H1A, H1B, H1C, H1D, H1E, and H1T. It is likely that this difference in amino acid sequences accounts for the functional difference. Although H1T is mapped relatively closer to H1A, H1B, H1C, H1D, and H1E than H1FOO is, H1T branches from the cluster of these somatic variants. This difference might contribute to the consistency of H1T in the case of nucleolar accumulation and its preference for rDNA. The preference for rDNA is also observed in linker histone of unicellular organisms that possess only one linker histone variant; in *Saccharomyces cerevisiae*, linker histone H1 represses recombination at rDNA,[49] and Hho1p in yeast is required for efficient rDNA transcription.[50] Considering these reports, H1T could be regarded as the most primitive variant among 10 mammalian H1 variants in that it inherited the characteristics of the preference for rDNA during evolutional expansion of H1 coding genes.

rDNA transcription is the first step of ribosomal biogenesis. In mammals, studies on the epigenetic regulation of rDNA transcription have mainly focused on DNA methylation and histone modification.[51,52] Our study revealed that the linker histone variant H1T functions to repress rDNA transcription by condensing rDNA chromatin structure. These findings on this specific H1 variant will open a new aspect of epigenetic studies on rDNA transcription.

Materials and methods

Reagents

Reagents without specific references to suppliers were purchased from Wako. All restriction enzymes used in this study were purchased from Takara. All primers were prepared by SIGMA-ALDRICH. Primer sequences are shown in Table S1. The composition of the medium used for cell culture is shown in Table S2. Antibodies were listed in Table S3.

The experiments described in the present study were repeated, at least, three times with similar results in each case. The results shown are representative for all repeated experiments.

Cell culture

AGS, HSC-39, and HSC-57 cell lines were kindly provided by Dr. Toshikazu Ushijima at the National Cancer Center. MCF-7 and YMB-1 cell lines were provided by the National Institute of

Biomedical Innovation. The MDA-MB-231 cell line, MBECs and MLECs were purchased from ATCC. KATOIII and HuTu80 cell lines were provided by the RIKEN BRC through the National Bio-Resource Project of the MEXT. hRPTECs, HAECs, and SkMCs were purchased from Lonza. ES cells (J1 line), which were derived from the 129S4/SvJae mouse embryo, were kindly provided by Dr. En Li.[53]

Tissue collection and isolation of spermatogenic cells

Testes were collected from 13-week-old C57BL/6N male mice (Charles River Japan). Spermatogenic cells were isolated from the testes of 6-week-old ICR mice (Charles River Japan) as described previously.[54] After the Sertoli cells were removed using cell strainers, the isolated spermatogenic cells were sampled in gel on a glass slide using Smear Gell (GenoStaff, SG-01) for fluorescent immunostaining. The experiments were performed according to the guidelines for the care and use of laboratory animals (Graduate School of Agriculture and Life Sciences, the University of Tokyo).

RNA extraction and cDNA synthesis

Total RNA from cultured cells was isolated using TRIZOL reagent (Invitrogen, 15596-018), the RNeasy Plus Micro Kit (Qiagen, 74034), or the Direct-zol RNA MiniPrep Kit (Zymo Research, R2052) according to each manufacturer's instructions. Total RNA-Stomach, Human (R1234248-50) and Total RNA-Testis, Human (R1234260-50) were purchased from Como Bio Co., Ltd. First-strand cDNA was synthesized from total RNA by using oligo(dT)20 primers and the SuperScript III First-Strand Synthesis System (Invitrogen, 18080-085). For measurement of pre-rRNA expression, cDNA samples were obtained using random hexamers (Invitrogen, N8080127).

RT-PCR and quantitative PCR (qPCR)

PCR amplification of cDNA was conducted with GoTaq Flexi DNA Polymerase (Promega, M8296). Amplification conditions were as follows: denaturation at 95°C for 3 min; appropriate number of cycles of 95°C for 30 sec, 60°C for 30 sec, and 72°C for 15 sec; and a final extension step at 72°C for 30 sec. RT-PCR products were subjected to electrophoresis on a 2% agarose gel with GelRed fluorescence dye (Biotium, 41003). The number of PCR cycles for each gene is shown in the figures for each experiment.

Each quantitative PCR (qPCR) was performed with THUNDERBIRD SYBR qPCR Mix (Toyobo, QPS-101) using the Light Cycler 96 (Roche) or the ABI7500 thermal cycler (Applied Biosystems). Amplification conditions were as follows: 95°C for 1 min; 40 cycles of 95°C for 15 sec and 60°C for 35 sec; and dissociation steps of 95°C for 15 sec, 60°C for 1 min, 95°C for 15 sec, and 60°C for 15 sec. Experiments were carried out in triplicate. qPCR was also carried out with a high throughput gene expression platform based on microfluidic dynamic arrays (Fluidigm) as previous report.[15] The Student's t-test was utilized for statistical analysis.

Protein extraction and western blotting

Insoluble nuclear fractions were collected using LysoPure Nuclear and Cytoplasmic Extractor Kit (295-73901). Isolated proteins were resolved on a 20% SDS-PAGE gel and transferred to an Immobilon PVDF membrane (Merk Millipore, IPVH304F0). The membrane was blocked with 5% skim milk solution in 0.1% Tween 20 in TBS (TBS-T) at room temperature (RT) for 1 hr and rinsed 3 times with TBS-T before incubation with the primary antibody diluted in 1% BSA in TBS-T at 4°C overnight. After incubation, the membrane was rinsed 3 times with TBS-T and was incubated with the HRP-conjugated secondary antibody (1:5000, diluted with 1% BSA in TBS-T) at RT for 1 hr. After rinsing the membrane 3 times with TBS-T, protein bands were detected using SuperSignal West Pico (Thermo, 34080).

Preparation of polyclonal antibody against H1T

The part of the human H1T gene encoding the amino acid sequence of H1T (AA115-207) was amplified by PCR from cDNA of human iPS cells using PrimeSTAR HS DNA Polymerase (Takara, R010A) according to manufacturer's instructions. The forward and reverse primers contained *Nhe*I and *Bam*HI restriction sites, respectively. The PCR product was inserted into a pGEM-T Easy vector (Promega, A1360) and the presence of the appropriate insert was confirmed by BigDye Terminator v3.1 Cycle Sequencing Kit (Applied Biosystems, 4337455).

The pGEM-T Easy vector containing collective insert was double digested by *Nhe*I/*Bam*HI and then ligated into a *Nhe*I/*Bam*HI-linearized pET-28b vector (Merck Millipore, 69,865). The *E. coli* Rosetta 2 competent cells containing the recombinant plasmids were grown at 37°C. After 16 hr of the culture, the expression of recombinant protein was induced by supplementation of 1.19 μg/mL IPTG. Cells were suspended in buffer-urea (20 mM Na-phosphate, 0.5 M NaCl, 0.5 M imidazole, and 8 M urea) and His-tagged proteins were collected from the cell-free extract by using Ni^{2+}–nitrilotriacetate resin (Qiagen, 30,210) and eluted with buffer-imidazole (20 mM Na-Phosphate, 0.5 M NaCl, 5 mM Imidazole, and 8 M urea). The eluted proteins were dialyzed in PBS(−) containing 2 M urea at 4°C for overnight. A rabbit was injected with His-tagged recombinant H1T 3 times, and its serum was collected. Polyclonal antibody against H1T (α-H1T) was purified with CNBr-activated Sepharose 4B (GE Healthcare Life Sciences, 17-0430-01) with the recombinant H1T. Injection of antigen into rabbits and collection of the anti-serum were performed by GenoStaff Co. The α-H1T was confirmed to be able to use immunostaining, immunoprecipitation and protein gel blotting in human and mouse samples (Fig. S7).

Plasmids for overexpression and knockdown

Human full-length *H1A, H1B, H1C, H1D, H1E,* and *H1T* encoding cDNA was amplified using cDNA from AGS cells with 3xFlag-tagged by 2 PCR amplifications using PrimeSTAR HS DNA Polymerase (Takara, R010A) or PrimeSTAR Max (Takara, R045A), and then ligated into the pENTR/D-TOPO

vector (Life Technologies, K240020SP) and the appropriate inserts were confirmed by BigDye sequencing. 3xFlag-fused genes were subcloned into a pCAG-DEST-IRES-Blasticidin-pA vector, which was generated by using a combination of the Gateway Vector Conversion System (Invitrogen, 11828-029) and pPyCAG-BstXI-IB (RIKEN BRC DNA BANK, RDB12107), by Gateway LR Clonase (Invitrogen, 11,791,019).

For the H1T knockdown (K_D), two specific miRNA sequences targeting the open reading frame of H1T were cloned into the pcDNA 6.2-GW/EmGFP-miR vector (Thermo Fisher Scientific, K493600). Similarly, a sequence targeting the LacZ-encoding mRNA was cloned and denoted control-miR.

Transfection of plasmids and establishment of knockdown/overexpressing cell lines

Plasmids were purified using the Quantum Prep Plasmid Midi Prep Kit (BIO-RAD), followed by phenol chloroform isoamyl alcohol extraction and ethanol precipitation. Plasmids were transfected into AGS cells by Lipofectamine 2000 (Life Technologies, 11,668,019). Plasmids were transfected into MDA-MB-231 cells using the Neon Transfection System (Invitrogen, MPK10096) or ScreenFect A (293-73201) according to the manufacturer's protocol. In MCF-7 cells, transfection was performed by jetPRIME (Polyplus-transfection, 114-15). Cells were selected with 2 μg/mL blasticidin after 24 hr of the transfection. For the establishment of knockdown/overexpressing cell lines, cells were transfected with linearized vectors and were subjected to limiting dilution to obtain single-cell derived colonies.

Fluorescent immunostaining

Adhesive cells cultured in 4-well dishes containing gelatin-coated coverslips were fixed with 4% paraformaldehyde in PBS ($-$) at RT for 20 min. Floating cells (HSC-39) and mouse spermatogenic cells were sampled in gel on slide glass using Smear Gell (GenoStaff, SG-01) according to the standard protocol and then fixed with 10% Formaldehyde Neutral Buffer Solution (NACALAI, 37152-51) at RT for 20 min. After fixation, samples were permeabilized with 0.1% Triton X-100 in PBS($-$) at RT for 30 min followed by incubation with blocking buffer (5% BSA-0.1% Tween 20) in PBS($-$) at 4°C overnight and were incubated with primary antibodies diluted in blocking buffer at 4°C overnight. After three washes with wash buffer (0.1% Tween 20 in PBS($-$)), samples were incubated with secondary antibodies diluted in blocking buffer at RT for 1 hr and then the nuclei were stained with DAPI solution (DOJINDO, 340-07971) diluted in PBS($-$) at RT for 20 min. The coverslips were mounted with VECTASHIELD (Vector Laboratories, H-1000), and imaged using the confocal laser scanning microscope FV10i (OLYMPUS).

Immunohistochemistry in tissue sections

Frozen sections of mouse tissues were fixed in acetone for 10 min at 4°C. After washing with PBS($-$), the sections were treated with 0.3% hydrogen peroxide/methanol at RT for 30 min. After washing with TBS, the sections were blocked with G-Block (GenoStaff, GB-01) for 10 min at RT. After washing with TBS, the sections were also blocked with the Avidin/Biotin Blocking Kit (Vector Laboratories, SP-2001) according to the manufacturer's protocol. After washing with TBS, the sections were incubated with 10 μg/mL primary antibody solution at 4°C overnight. After multiple washes with TBS, the sections were incubated with anti-rabbit Ig biotin (Dako, E0432) at 1:600 dilution at RT for 30 min. After multiple washes with TBS, the sections were incubated with peroxidase-conjugated streptavidin (Nichirei, 426,062) at RT for 5 min. After multiple washes with TBS, sections were treated with DAB/H2O2, counterstained (hematoxylin), and mounted (xylene mounting medium). This immunohistochemistry was performed by GenoStaff Co.

Cell cycle synchronization

Cell cycle synchronization was performed according to the previous report.[55-57] Briefly, cell cycles of AGS cells were synchronized by two cycles of 2 mM thymidine treatment for 16 hr followed by an 8 hr incubation thymidine. After the double thymidine treatment, cells were treated with 2 mM thymidine (207-19421), 100 ng/mL nocodazole (140-08531), or 400 μM L-mimosine (Sigma-Aldrich, M0253) for 14 hr. After multiple washes with ice-cold PBS, cells were subjected to fluorescent immunostaining.

ChIP assay

The ChIP assay was performed with 1×10^7 cells per assay by using the ChIP-IT Express Shearing Kit (Active Motif, 53,032) according to the manufacturer's instructions. Briefly, fixed cells were lysed, and the chromatin was sheared using an enzymatic shearing cocktail for 10 min at 37°C. After IP, DNA was purified by ChIP DNA Clean and Concentrator (Zymo Research, D5205) and was subjected to ChIP-seq or qPCR.

ChIP-seq

The libraries for massive parallel sequencing were prepared with the TruSeq DNA Sample Preparation v2 Kit, Set A/B (Illumina, FC-121-2001/-2002) according to the manufacturer's instructions. Briefly, 50 ng of immunoprecipitated DNA or input DNA was end repaired, 3′ adenylated, and ligated with adapter oligos. DNA fragments within the range of 120-500 bp were purified using AMpure XP beads (Beckman Coulter, A63880) and amplified by PCR. Library DNA was electrophoresed on a 2% agarose gel and subsequently purified with a Zymoclean Gel DNA Recovery Kit (Zymo Research, D4007). Libraries were quantified by BioAnalyzer2000 (Agilent). Sequencing was performed with Illumina HiSeq 2000 systems, and raw sequence reads containing more than 30% of 'N' were removed, and adapter sequences were trimmed. Clean sequences were aligned against mammalian repeats from Repbase version 18.11[32] using BWA aligner software in the Galaxy platform (https://usegalaxy.org/). The percentage of reads for each repeat mapped to Repbase was calculated by dividing reads mapped to the respective repeat by the total reads in the library, and the input ration for the respective repeat was subsequently calculated as the ratio of the percent of reads of ChIP-

seq library to that of the input-seq library. Sequencing data of H1T are available at GEO with accession numbers GSE75287. Sequencing data of human and mouse somatic variants were cited from the previous reports with accession number GSE49345 and GSE46134, respectively.[29,33]

Nuclease sensitivity assay

For DNase I sensitivity assay, AGS, MDA-MB-231, and MCF-7 cells were analyzed by using EZ Nucleosomal DNA Prep Kit (Zymo Research, D5220) according to the manufacturer's instructions, with a minor modification. Briefly, 1×10^6 cells were suspended in 100 μL of Atlantis Digestion Buffer and were digested with 1 U of RQ1 DNase (Promega, M6101) by incubation at 37°C for 30 min. For MNase digestion, 1×10^6 cells were suspended in 100 μL of MN Digestion Buffer and digested with 0.01 U of microccocal nuclease by incubation at 37°C for 8 min. Purified DNA samples were subjected to qPCR.

Image processing

For measurement of size and number of nucleoli, merged immunofluorescence images of DAPI (blue) and B23 (red) were processed using the CellProfiler software (http://www.cellprofiler.org/) based on the previous report.[58] The Wilcoxon rank-sum test was utilized for statistical analysis.

Accession number

Sequencing data have been deposited in the NCBI's Gene Expression Omnibus (GEO)[59] under GEO Series accession number GSE75287.

Disclosure of potential conflicts of interest

No potential conflicts of interest were disclosed.

Authors' contributions

The author contributions are as follows: K.H. designed this study; the study was discussed with S.T. and K.S; R.T. and K.H. performed experiments; R.T., K.H., S.T. and K.S. prepared the manuscript.

References

1. Finch JT, Klug A. Solenoidal model for superstructure in chromatin. Proc Natl Acad Sci U S A 1976; 73:1897-901; PMID:1064861; http://dx.doi.org/10.1073/pnas.73.6.1897

2. Simpson RT. Structure of the chromatosome, a chromatin particle containing 160 base pairs of DNA and all the histones. Biochemistry 1978; 17:5524-31; PMID:728412; http://dx.doi.org/10.1021/bi00618a030

3. Kasinsky HE, Lewis JD, Dacks JB, Ausió J. Origin of H1 linker histones. FASEB J 2001; 15:34-42; PMID:11149891; http://dx.doi.org/10.1096/fj.00-0237rev

4. Khochbin S. Histone H1 diversity: bridging regulatory signals to linker histone function. Gene 2001; 271:1-12; http://dx.doi.org/10.1016/S0378-1119(01)00495-4

5. Happel N, Doenecke D. Histone H1 and its isoforms: contribution to chromatin structure and function. Gene 2009; 431:1-12; PMID:19059319; http://dx.doi.org/10.1016/j.gene.2008.11.003

6. Kowalski A, Pałyga J. Linker histone subtypes and their allelic variants. Cell Biol Int 2012; 36:981-96; PMID:23075301; http://dx.doi.org/10.1042/CBI20120133

7. Tanaka M, Hennebold JD, Macfarlane J, Adashi EY. A mammalian oocyte-specific linker histone gene H1oo: homology with the genes for the oocyte-specific cleavage stage histone (cs-H1) of sea urchin and the B4/H1M histone of the frog. Development 2001; 128:655-64; PMID:11171391

8. Tanaka M, Kihara M, Meczekalski B, King GJ, Adashi EY. H1oo: a pre-embryonic H1 linker histone in search of a function. Mol Cell Endocrinol 2003; 202:5-9; PMID:12770723; http://dx.doi.org/10.1016/S0303-7207(03)00054-6

9. Branson RE, Grimes SR, Yonuschot G, Irvin JL. The histones of rat testis. Arch Biochem Biophys 1975; 168:403-12; PMID:1094956; http://dx.doi.org/10.1016/0003-9861(75)90269-6

10. Bucci LR, Brock WA, Meistrich ML. Distribution and synthesis of histone 1 subfractions during spermatogenesis in the rat. Exp Cell Res 1982; 140:111-8; PMID:7106196; http://dx.doi.org/10.1016/0014-4827(82)90162-8

11. Martianov I, Brancorsini S, Catena R, Gansmuller A, Kotaja N, Parvinen M, Sassone-Corsi P, Davidson I. Polar nuclear localization of H1T2, a histone H1 variant, required for spermatid elongation and DNA condensation during spermiogenesis. Proc Natl Acad Sci U S A 2005; 102:2808-13; PMID:15710904; http://dx.doi.org/10.1073/pnas.0406060102

12. Yan W, Ma L, Burns KH, Matzuk MM. HILS1 is a spermatid-specific linker histone H1-like protein implicated in chromatin remodeling during mammalian spermiogenesis. Proc Natl Acad Sci USA 2003; 100:10546-51; PMID:12920187; http://dx.doi.org/10.1073/pnas.1837812100

13. Bustin M, Catez F, Lim JH. The dynamics of histone H1 function in chromatin. Mol Cell 2005; 17:617-20; PMID:15749012; http://dx.doi.org/10.1016/j.molcel.2005.02.019

14. Woodcock CL, Skoultchi AI, Fan Y. Role of linker histone in chromatin structure and function: H1 stoichiometry and nucleosome repeat length. Chromosome Res 2006; 14:17-25; PMID:16506093; http://dx.doi.org/10.1007/s10577-005-1024-3

15. Hayakawa K, Ohgane J, Tanaka S, Yagi S, Shiota K. Oocyte-specific linker histone H1foo is an epigenomic modulator that decondenses chromatin and impairs pluripotency. Epigenetics 2012; 7:1029-36; PMID:22868987; http://dx.doi.org/10.4161/epi.21492

16. Bradbury EM, Chapman GE, Danby SE, Hartman PG, Riches PL. Studies on the role and mode of operation of the very-lysine-rich histone H1 (F1) in eukaryote chromatin. The properties of the N-terminal and C-terminal halves of histone H1. Eur J Biochem 1975; 57:521-8; PMID:1175657; http://dx.doi.org/10.1111/j.1432-1033.1975.tb02327.x

17. Hartman PG, Chapman GE, Moss T, Bradbury EM. Studies on the role and mode of operation of the very-lysine-rich histone H1 in eukaryote chromatin. The three structural regions of the histone H1 molecule. Eur J Biochem 1977; 77:45-51; PMID:908338; http://dx.doi.org/10.1111/j.1432-1033.1977.tb11639.x

18. Roque A, Ponte I, Suau P. Interplay between histone H1 structure and function. Biochim Biophys Acta 2015; PMID:26415976

19. Pérez-Montero S, Carbonell A, Azorín F. Germline-specific H1 variants: the "sexy" linker histones. Chromosoma 2015

20. Lennox RW, Cohen LH. The alterations in H1 histone complement during mouse spermatogenesis and their significance for H1 subtype function. Dev Biol 1984; 103:80-4; PMID:6714521; http://dx.doi.org/10.1016/0012-1606(84)90009-5

21. Steger K, Klonisch T, Gavenis K, Drabent B, Doenecke D, Bergmann M. Expression of mRNA and protein of nucleoproteins during human spermiogenesis. Mol Hum Reprod 1998; 4:939-45; PMID:9809674; http://dx.doi.org/10.1093/molehr/4.10.939

22. Drabent B, Bode C, Bramlage B, Doenecke D. Expression of the mouse testicular histone gene H1t during spermatogenesis. Histochem Cell Biol 1996; 106:247-51; PMID:8877387; http://dx.doi.org/10.1007/BF02484408

23. Drabent B, Bode C, Miosge N, Herken R, Doenecke D. Expression of the mouse histone gene H1t begins at premeiotic stages of spermatogenesis. Cell Tissue Res 1998; 291:127-32; PMID:9394050; http://dx.doi.org/10.1007/s004410050986

24. Lin Q, Sirotkin A, Skoultchi AI. Normal spermatogenesis in mice lacking the testis-specific linker histone H1t. Mol Cell Biol 2000; 20:2122-8; PMID:10688658; http://dx.doi.org/10.1128/MCB.20.6.2122-2128.2000

25. Lin Q, Inselman A, Han X, Xu H, Zhang W, Handel MA, Skoultchi AI. Reductions in linker histone levels are tolerated in developing spermatocytes but cause changes in specific gene expression. J Biol Chem 2004; 279:23525-35; PMID:15039436; http://dx.doi.org/10.1074/jbc.M400925200

26. Sancho M, Diani E, Beato M, Jordan A. Depletion of human histone H1 variants uncovers specific roles in gene expression and cell growth. PLoS Genet 2008; 4:e1000227; PMID:18927631; http://dx.doi.org/10.1371/journal.pgen.1000227

27. Suzuki M. SPKK, a new nucleic acid-binding unit of protein found in histone. EMBO J 1989; 8:797-804; PMID:2470589

28. Drabent B, Kardalinou E, Doenecke D. Structure and expression of the human gene encoding testicular H1 histone (H1t). Gene 1991; 103:263-8; PMID:1889752; http://dx.doi.org/10.1016/0378-1119(91)90284-I

29. Cao K, Lailler N, Zhang Y, Kumar A, Uppal K, Liu Z, Lee EK, Wu H, Medrzycki M, Pan C, et al. High-resolution mapping of h1 linker histone variants in embryonic stem cells. PLoS Genet 2013; 9:e1003417; PMID:23633960

30. Mayor R, Izquierdo-Bouldstridge A, Millán-Ariño L, Bustillos A, Sampaio C, Luque N, Jordan A. Genome distribution of replication-independent histone H1 variants shows H1.0 associated with nucleolar domains and H1X associated with RNA polymerase II-enriched regions. J Biol Chem 2015; 290:7474-91; PMID:25645921; http://dx.doi.org/10.1074/jbc.M114.617324

31. Németh A, Conesa A, Santoyo-Lopez J, Medina I, Montaner D, Péterfia B, Solovei I, Cremer T, Dopazo J, Längst G. Initial genomics of the human nucleolus. PLoS Genet 2010; 6:e1000889; PMID:20361057

32. Jurka J, Kapitonov VV, Pavlicek A, Klonowski P, Kohany O, Walichiewicz J. Repbase Update, a database of eukaryotic repetitive elements. Cytogenet Genome Res 2005; 110:462-7; PMID:16093699; http://dx.doi.org/10.1159/000084979

33. Millán-Ariño L, Islam AB, Izquierdo-Bouldstridge A, Mayor R, Terme JM, Luque N, Sancho M, López-Bigas N, Jordan A. Mapping of six somatic linker histone H1 variants in human breast cancer cells uncovers specific features of H1.2. Nucleic Acids Res 2014; 42:4474-93; PMID:24476918; http://dx.doi.org/10.1093/nar/gku079

34. Cong R, Das S, Douet J, Wong J, Buschbeck M, Mongelard F, Bouvet P. macroH2A1 histone variant represses rDNA transcription. Nucleic Acids Res 2014; 42:181-92; PMID:24071584; http://dx.doi.org/10.1093/nar/gkt863

35. Biggiogera M, Kaufmann SH, Shaper JH, Gas N, Amalric F, Fakan S. Distribution of nucleolar proteins B23 and nucleolin during mouse spermatogenesis. Chromosoma 1991; 100:162-72; PMID:1710179; http://dx.doi.org/10.1007/BF00337245

36. Shaw ML, Williams EJ, Hawes S, Saffery R. Characterisation of histone variant distribution in human embryonic stem cells by transfection of in vitro transcribed mRNA. Mol Reprod Dev 2009; 76:1128-42; PMID:19606468; http://dx.doi.org/10.1002/mrd.21077

37. Zheng Y, John S, Pesavento JJ, Schultz-Norton JR, Schiltz RL, Baek S, Nardulli AM, Hager GL, Kelleher NL, Mizzen CA. Histone H1 phosphorylation is associated with transcription by RNA polymerases I and II. J Cell Biol 2010; 189:407-15; PMID:20439994; http://dx.doi.org/10.1083/jcb.201001148

38. Stoldt S, Wenzel D, Schulze E, Doenecke D, Happel N. G1 phase-dependent nucleolar accumulation of human histone H1x. Biol Cell 2007; 99:541-52; PMID:17868027; http://dx.doi.org/10.1042/BC20060117

39. van der Bruggen P, Traversari C, Chomez P, Lurquin C, De Plaen E, Van den Eynde B, Knuth A, Boon T. A gene encoding an antigen recognized by cytolytic T lymphocytes on a human melanoma. Science 1991; 254:1643-7; PMID:1840703; http://dx.doi.org/10.1126/science.1840703

40. De Plaen E, Arden K, Traversari C, Gaforio JJ, Szikora JP, De Smet C, Brasseur F, van der Bruggen P, Lethé B, Lurquin C, et al. Structure, chromosomal localization, and expression of 12 genes of the MAGE family. Immunogenetics 1994; 40:360-9; PMID:7927540; http://dx.doi.org/10.1007/BF01246677

41. Fratta E, Coral S, Covre A, Parisi G, Colizzi F, Danielli R, Nicolay HJ, Sigalotti L, Maio M. The biology of cancer testis antigens: putative function, regulation and therapeutic potential. Mol Oncol 2011; 5:164-82; PMID:21376678; http://dx.doi.org/10.1016/j.molonc.2011.02.001

42. Whitehurst AW. Cause and consequence of cancer/testis antigen activation in cancer. Annu Rev Pharmacol Toxicol 2014; 54:251-72; PMID:24160706; http://dx.doi.org/10.1146/annurev-pharmtox-011112-140326

43. Pianese G. Beitrag zur Histologie und Aetiologie der Carcinoma. Histologische und experimentelle Untersuchungen. Beitr Pathol Anat Allg Pathol 1896; 142: 1-193.

44. Derenzini M, Montanaro L, Treré D. What the nucleolus says to a tumour pathologist. Histopathology 2009; 54:753-62; PMID:19178588; http://dx.doi.org/10.1111/j.1365-2559.2008.03168.x

45. Green R, Noller HF. Ribosomes and translation. Annu Rev Biochem 1997; 66:679-716; PMID:9242921; http://dx.doi.org/10.1146/annurev.biochem.66.1.679

46. Bacalini MG, Pacilli A, Giuliani C, Penzo M, Treré D, Pirazzini C, Salvioli S, Franceschi C, Montanaro L, Garagnani P. The nucleolar size is associated to the methylation status of ribosomal DNA in breast carcinomas. BMC Cancer 2014; 14:361; PMID:24884608; http://dx.doi.org/10.1186/1471-2407-14-361

47. Monesi V. Synthetic activities during spermatogenesis in the mouse RNA and protein. Exp Cell Res 1965; 39:197-224; PMID:5318974; http://dx.doi.org/10.1016/0014-4827(65)90023-6

48. Kierszenbaum AL, Tres LL. Structural and transcriptional features of the mouse spermatid genome. J Cell Biol 1975; 65:258-70; PMID:1127016; http://dx.doi.org/10.1083/jcb.65.2.258

49. Li C, Mueller JE, Elfline M, Bryk M. Linker histone H1 represses recombination at the ribosomal DNA locus in the budding yeast Saccharomyces cerevisiae. Mol Microbiol 2008; 67:906-19; PMID:18179596; http://dx.doi.org/10.1111/j.1365-2958.2007.06101.x

50. Levy A, Eyal M, Hershkovits G, Salmon-Divon M, Klutstein M, Katcoff DJ. Yeast linker histone Hho1p is required for efficient RNA polymerase I processivity and transcriptional silencing at the ribosomal DNA. Proc Natl Acad Sci U S A 2008; 105:11703-8; PMID:18687885; http://dx.doi.org/10.1073/pnas.0709403105

51. McStay B, Grummt I. The epigenetics of rRNA genes: from molecular to chromosome biology. Annu Rev Cell Dev Biol 2008; 24:131-57; PMID:18616426; http://dx.doi.org/10.1146/annurev.cellbio.24.110707.175259

52. Guetg C, Santoro R. Formation of nuclear heterochromatin: the nucleolar point of view. Epigenetics 2012; 7:811-4; PMID:22735386; http://dx.doi.org/10.4161/epi.21072

53. Li E, Bestor TH, Jaenisch R. Targeted mutation of the DNA methyl-transferase gene results in embryonic lethality. Cell 1992; 69:915-26; PMID:1606615; http://dx.doi.org/10.1016/0092-8674(92)90611-F

54. Chang YF, Lee-Chang JS, Panneerdoss S, MacLean JA, Rao MK. Isolation of Sertoli, Leydig, and spermatogenic cells from the mouse testis. Biotechniques 2011; 51:341-2, 4; PMID:22054547; http://dx.doi.org/10.2144/000113764

55. Liu SI, Chi CW, Lui WY, Mok KT, Wu CW, Wu SN. Correlation of hepatocyte growth factor-induced proliferation and calcium-activated potassium current in human gastric cancer cells. Biochim Biophys Acta 1998; 1368:256-66; PMID:9459603; http://dx.doi.org/10.1016/S0005-2736(97)00183-1

56. Petrocca F, Visone R, Onelli MR, Shah MH, Nicoloso MS, de Martino I, Iliopoulos D, Pilozzi E, Liu CG, Negrini M, et al. E2F1-regulated microRNAs impair TGFbeta-dependent cell-cycle arrest and apoptosis in gastric cancer. Cancer Cell 2008; 13:272-86; PMID:18328430; http://dx.doi.org/10.1016/j.ccr.2008.02.013

57. Qu Y, Li JF, Cai Q, Wang YW, Gu QL, Zhu ZG, Liu BY. Over-expression of FRZB in gastric cancer cell suppresses proliferation and induces differentiation. J Cancer Res Clin Oncol 2008; 134:353-64; PMID:17680269; http://dx.doi.org/10.1007/s00432-007-0291-0

58. Lamprecht MR, Sabatini DM, Carpenter AE. CellProfiler: free, versatile software for automated biological image analysis. Biotechniques 2007; 42:71-5; PMID:17269487; http://dx.doi.org/10.2144/000112257

59. Edgar R, Domrachev M, Lash AE. Gene Expression Omnibus: NCBI gene expression and hybridization array data repository. Nucleic Acids Res 2002; 30:207-10; PMID:11752295; http://dx.doi.org/10.1093/nar/30.1.207